

Universality in coupled stochastic Burgers systems with degenerate flux Jacobian

Dipankar Roy

International Centre for Theoretical Sciences, Tata Institute of Fundamental Research, Bangalore 560089, India

Abhishek Dhar

International Centre for Theoretical Sciences, Tata Institute of Fundamental Research, Bangalore 560089, India

Konstantin Khanin

Department of Mathematics, University of Toronto, 40 St George Street, Toronto, ON M5S 2E4, Canada

Manas Kulkarni

International Centre for Theoretical Sciences, Tata Institute of Fundamental Research, Bangalore 560089, India

Herbert Spohn

Zentrum Mathematik and Physik Department, Technische Universität München, Garching 85748, Germany

Abstract. In our contribution we study stochastic models in one space dimension with two conservation laws. One model is the coupled continuum stochastic Burgers equation, for which each current is a sum of quadratic non-linearities, linear diffusion, and spacetime white noise. The second model is a two-lane stochastic lattice gas. As distinct from previous studies, the two conserved densities are tuned such that the flux Jacobian, a 2×2 matrix, has coinciding eigenvalues. In the steady state, investigated are spacetime correlations of the conserved fields and the time-integrated currents at the origin. For a particular choice of couplings the dynamical exponent $3/2$ is confirmed. Furthermore, at these couplings, continuum stochastic Burgers equation and lattice gas are demonstrated to be in the same universality class.

Contents

1	Introduction	3
2	Coupled stochastic Burgers equations, cyclicity condition	5
2.1	One component	5
2.2	Two components	6
2.3	Time-invariance	8
2.4	Cyclic matrices	9
2.5	Scaling hypothesis	10
2.6	Models to be studied	11
3	Numerical simulations of coupled stochastic Burgers and KPZ equations	11
4	Two-lane lattice gas	15
5	Numerical simulations of the two-lane lattice gas	19
6	Universality	22
7	Mode-coupling theory	24
8	Discussions	27
9	Summary and Outlook	28
Appendix A		
	Transforming \vec{G} -matrices	29
Appendix B		
	Further results for the two-lane model	29
	Appendix B.1	
	Cyclicity	29
	Appendix B.2	
	Uniqueness of the umbilic point	29
Appendix C		
	Symmetric and anti-symmetric combinations	30

1. Introduction

In the context of the one-dimensional Kardar-Parisi-Zhang (KPZ) equation governing surface growth [1, 2, 3], there is a long standing interest in stochastic models with a single conservation law. A prototypical example is the continuum stochastic Burgers equation which describes the motion of KPZ slopes. Further examples are lattice gases, such as ASEP [4], TASEP [5, 6, 7], PNG [8], and more. The extension to several components was largely triggered by the observation that the linear Landau-Lifshitz fluctuation theory fails for one-dimensional fluids. These classical particle systems generically have three conservation laws and the appropriate nonlinear version of the fluctuation theory is a continuum stochastic Burgers equation with three components [9]. The analysis of these equations relies on the fact that the heat peak and sound peaks have distinct velocities. More recently, as a great surprise, signatures of KPZ physics were also observed in the spin-spin spacetime correlations of the isotropic spin- $\frac{1}{2}$ chain at high temperatures [10, 11, 12, 13]. In [14] an effective theory for spin and helicity has been derived. The dynamical equations are two coupled continuum Burgers equations. As a very particular feature, in this case there are no sound modes and the standing still heat peak has two components, which leads to more intricate correlation effects and is not covered by the conventional analysis of nonlinear fluctuating hydrodynamics [9]. For us, this is one of the motivation to study more systematically stochastic Burgers systems, both continuum and lattice, with a degenerate flux Jacobian.

For a single conserved field many detailed studies are available. Progress up to 2015 is discussed in the Les Houches lectures [15]. Surprising properties have been uncovered. Their experimental realization is reviewed in an instructive article by K. Takeuchi [16]. In this contribution, we will focus on coupled stochastic continuum Burgers equations and lattice gases in one dimension with two conserved densities, u_1 and u_2 . To understand properties of their spacetime dependent structure function the flux Jacobian is a central quantity. To provide a definition, we denote by $j_1(u_1, u_2)$ and $j_2(u_1, u_2)$ the currents, averaged in a spatially homogeneous steady state, in dependence on the densities $\vec{u} = (u_1, u_2)$. The flux Jacobian is then the 2×2 matrix

$$A_{\alpha\beta}(\vec{u}) = \partial_{u_\beta} j_\alpha(\vec{u}), \tag{1.1}$$

$\alpha, \beta = 1, 2$. More explicitly, the flux Jacobian takes the form

$$A = \begin{pmatrix} \partial_{u_1} j_1 & \partial_{u_2} j_1 \\ \partial_{u_1} j_2 & \partial_{u_2} j_2 \end{pmatrix}. \tag{1.2}$$

This matrix depends on \vec{u} and is not symmetric, in general. However, A has always real eigenvalues and a complete system of left and right eigenvectors [17, 18, 9]. If the lattice

gas is prepared in a statistically stationary spatially homogeneous state, then an initial perturbation at the origin will generate two localized peaks travelling with velocities given by the eigenvalues of A . If A is non-degenerate, for long times, the peaks are spatially far apart and one argues that the two propagating modes reduce to the case of a single component [19, 20, 9]. The fine structure of these peaks depends on the second order expansion of the currents and is handled by nonlinear fluctuating hydrodynamics. For generic values of \vec{u} the matrix A will be non-degenerate. But there could be special points at which A is degenerate. Then the peaks travel with the same velocity and the decoupling approximation fails. The understanding of this case is the primary agenda of our investigation.

An early contribution is the study by Ertaş and Kardar [21], see also [22], who consider the dynamics of a stretched string, e.g. a vortex line, in a spacetime random medium. For the two transversal components they write two coupled stochastic differential equations of KPZ type and argue on physical grounds that the flux Jacobian (1.2) vanishes. Ertaş and Kardar report on numerical findings on scaling exponents for their coupled stochastic equations [22]. Given the fact that our understanding of one-component systems has significantly advanced since then [3, 23, 16], it is worthwhile to reconsider the two-component case with degenerate flux Jacobian, in particular to move beyond scaling exponents.

More recently revived interest has been initiated through the study of spin chains, both classical [24, 25, 26, 27] and quantum [10, 11, 28]. The KPZ exponent $3/2$ was theoretically established and experimentally confirmed [12, 13, 29]. Surprisingly, theoretical studies [11, 25, 26, 27] have also found that the spacetime spin-spin correlator shows a scaling function remarkably close to the exact solution from the one-component stationary KPZ equation. In an attempt to understand such features a coarse-grained description for the dynamics of spin and helicity density has been derived in [14]. The resulting model is stochastic and has the form of a two-component stochastic Burgers equation with degenerate flux Jacobian.

In our contribution, we report on numerical studies of continuum stochastic Burgers equations with two components, in which case degeneracy of the flux Jacobian is easily implemented. We also investigate a stochastic lattice gas with two lanes [30] and notice a remarkable universality between lattice and continuum systems. In the lattice gas, the particles stay in their own lane, hence the lane densities are conserved. The interaction arises through jump rates depending on the respective occupations in the other lane. At densities $u_1 = \frac{1}{2} = u_2$, the flux Jacobian turns out to be degenerate. In the continuum and lattice models the spatially homogeneous stationary state is known explicitly. We then investigate the spacetime covariance, a 2×2 matrix, of the conserved fields in the stationary state. Studied is also the time-integrated current through the origin, which is

a random two-vector, up to a term linear in time. For a single component, the scaling form of both observables is known rigorously and our task is to elucidate their extension to two components.

The paper is organized as follows. In Section 2, we discuss continuum coupled stochastic Burgers equations and study the cyclicity condition, ensuring a time-stationary measure which is Gaussian. The two-lane lattice model is introduced in Section 4 and its intriguing connection to coupled Burgers equations is established. Our numerical results on a discretized version of the two-component stochastic Burgers equation are presented in Section 3, while the Monte-Carlo results for the two-lane stochastic lattice gas model are provided in Section 5. Universality is taken up in Section 6. We also recall in Section 7 the mode-coupling theory for two-component stochastic Burgers equations. A more detailed comparison to prior work, discussion points, and summary can be found towards the end of the article. Some computations are relegated to the appendices.

2. Coupled stochastic Burgers equations, cyclicity condition

As starting point of our investigations we consider two coupled Langevin equations of stochastic Burgers type. The well-understood case of one component is briefly recalled. To have a concrete set-up for two components, the focus in this section is primarily on time-stationary steady states and on linear transformations of the two random density fields.

2.1. One component

The stochastic Burgers equation with a single component reads

$$\partial_t \phi(x, t) - \partial_x \left(a \phi(x, t) + \lambda \phi(x, t)^2 + d \partial_x \phi(x, t) + b \xi(x, t) \right) = 0. \quad (2.1)$$

Here $\phi(x, t)$ is the density field and $\xi(x, t)$ is standard spacetime Gaussian white noise,

$$\langle \xi(x, t) \xi(x', t') \rangle = \delta(x - x') \delta(t - t'). \quad (2.2)$$

In analysing the Langevin equation (2.1), a major simplification results from the knowledge of the time-stationary measures. In fact, these are Gaussian measures with arbitrary mean and covariance $\chi \delta(x - x')$. The susceptibility χ is determined by

$$\chi = b^2 / 2d. \quad (2.3)$$

To be noted, χ does not depend on the strength of the quadratic nonlinearity. Shifting the field ϕ by a constant as $\phi + \kappa_0$ merely modifies a as $a + 2\lambda\kappa_0$. In turn the linear

term can be removed by a Galilei transformation. Thus we can set $\mathbf{a} = 0$ and $\langle \phi(x) \rangle = 0$, average in the spatially homogeneous steady state.

The observable of interest is the spacetime correlator

$$\mathcal{S}(x, t) = \langle \phi(x, t) \phi(0, 0) \rangle, \quad (2.4)$$

which, because of the conservation law, satisfies the sum rule

$$\int_{\mathbb{R}} dx \mathcal{S}(x, t) = \chi. \quad (2.5)$$

Asymptotically $\mathcal{S}(x, t)$ is of scaling form. To determine the relation between space and time, one rescales $\phi(x, t)$. As a result the dynamical exponent z takes the value $z = 3/2$. Diffusion and noise term are sub-leading, but ensure local time-stationarity. For the correlator these considerations imply the scaling form

$$\mathcal{S}(x, t) = \chi t^{-2/3} g(t^{-2/3} x). \quad (2.6)$$

for large x, t . The integral of g equals one and the prefactor ensures the validity of Eq. (2.5).

As one important discovery from 2004 [31], the scaling function can be computed exactly with the result

$$\mathcal{S}(x, t) \simeq \chi (\Gamma_{\parallel} t)^{-2/3} f_{\text{KPZ}}\left((\Gamma_{\parallel} t)^{-2/3} x\right) \quad (2.7)$$

with $\Gamma_{\parallel} = 2|\lambda|\sqrt{2\chi}$. A numerical plot of the function f_{KPZ} can be found in [31]. The KPZ scaling theory claims that Eq. (2.7) holds for a wide range of stochastic particle models with a single conservation law, where χ is the static susceptibility and $\lambda = j''(\rho)/2$ with $j(\rho)$ the steady state average current. In this sense f_{KPZ} is a universal function and Γ_{\parallel} a very specific model-dependent parameter. In fact, the scaling (2.7) was originally obtained for the polynuclear growth model and later confirmed for the TASEP [32]. For the continuum stochastic Burgers equation (2.1), the scaling (2.7) was proved only eight years later [33].

2.2. Two components

The formal extension of Eq. (2.1) to two components becomes

$$\partial_t \phi_{\alpha} - \partial_x \left(A_{\alpha\beta} \phi_{\beta} + \langle \vec{\phi}, G^{\alpha} \vec{\phi} \rangle + D_{\alpha\beta} \partial_x \phi_{\beta} + B_{\alpha\beta} \xi_{\beta} \right) = 0, \quad (2.8)$$

$\alpha = 1, 2$, where ξ_1, ξ_2 are independent standard white noise components and G^1, G^2 are constant 2×2 matrices, which are symmetric by construction. Here and below, we use the

Einstein convention for summing over repeated Greek indices, i.e. summing over $\beta = 1, 2$ above. Sometimes it is convenient to use vector notation as

$$\vec{\phi} = (\phi_1, \phi_2), \quad \vec{\xi} = (\xi_1, \xi_2), \quad \vec{G} = (G^1, G^2). \quad (2.9)$$

In Eq. (2.8), the symbol $\langle \cdot, \cdot \rangle$ then refers the scalar product for 2-vectors and A, D, B, G^α are constant 2×2 matrices. For the degenerate case of interest, $A = c_0 1$ and c_0 can be set to zero through a Galilei transformation. Hence we set $A = 0$.

As in the case of a single component, one would like to determine the time-stationary measure. Since the system is nonlinear and does not satisfy detailed balance, no generic tools are available. One way out is to study the reverse question. We first fix a Gaussian measure with mean zero and covariance

$$\langle \phi_\alpha(x) \phi_{\alpha'}(x') \rangle = C_{\alpha\alpha'} \delta(x - x'), \quad (2.10)$$

where C is a symmetric strictly positive definite 2×2 matrix. As a generalization of Eq. (2.3), for the linear part of the coupled equation one has the relation

$$DC + CD^T = BB^T \quad (2.11)$$

with T denoting transpose. The Gaussian measure with covariance (2.10) is time-stationary in case $\vec{G} = 0$. Therefore we view C as given, but still allowing for some freedom of how to choose the matrices B, D . However, the linear part should have good mixing properties, which is ensured by $BB^T > 0$ and hence also $D + D^T > 0$. The issue is now to determine for which couplings \vec{G} the Gaussian measure remains time-stationary. This question can be resolved and we first state the result. One defines

$$\hat{G}^\alpha = (C^{-1})_{\alpha\beta} G^\beta. \quad (2.12)$$

The matrices \hat{G}^α are called *cyclic*, if they satisfy the *cyclicity* condition

$$\hat{G}_{\beta\gamma}^\alpha = \hat{G}_{\alpha\beta}^\gamma \quad (= \hat{G}_{\beta\alpha}^\gamma), \quad (2.13)$$

the latter identity being satisfied by construction. If \hat{G} is cyclic, then the Gaussian measure with covariance (2.10) is time-stationary.

As for one component, the Gaussians shifted by a constant field are still time-stationary. This is then equivalent to zero mean with an additional linear term, which is generically non-degenerate. To ensure a degenerate flux Jacobian, we therefore always assume zero mean for the Gaussian measure and also $A = 0$, as before. Of interest is then the spacetime correlator

$$S_{\alpha\beta}(x, t) = \langle \phi_\alpha(x, t) \phi_\beta(0, 0) \rangle. \quad (2.14)$$

S satisfies the sum rule

$$\int_{\mathbb{R}} dx S(x, t) = C. \quad (2.15)$$

Repeating the scaling argument for a single component, one concludes that the dynamical exponent still equals $3/2$. Thus for each matrix element one would expect a similar scaling as in Eq. (2.6). But now no exact solution is of help and in our contribution we will barely scratch the surface. For sure, there are exceptional \vec{G} matrices which lead to a different dynamical exponent. A trivial example would be $G_{11}^1 = 1$ and all other matrix elements 0. Then there will be a diffusive mode and a KPZ mode. Within the class of cyclic matrices we will formulate a conjecture which identifies those couplings having a dynamical exponent $3/2$.

2.3. Time-invariance

While one could study directly the continuum theory [34], the argument becomes more transparent by switching to the lattice, $j = 1, \dots, N$, with periodic boundary conditions and denoting the discretized field by $\phi_{j,\alpha}$, $\alpha = 1, 2$, see [35]. This discretization will also be used in our numerical simulations. The discretization of the linear part of Eq. (2.8) is standard and reads

$$\frac{d}{dt}\phi_{j,\alpha} = D_{\alpha\beta}(\phi_{j+1,\beta} - 2\phi_{j,\beta} + \phi_{j-1,\beta}) + B_{\alpha\beta}(\xi_{j,\beta} - \xi_{j-1,\beta}). \quad (2.16)$$

Condition (2.11) is imposed and $\{\xi_{j,\beta}(t)\}$ is a family of independent standard white noises in time. The time-stationary measure for the linear Langevin equation is the Gaussian

$$\prod_{j=1}^N \prod_{\alpha'=1}^2 \left((2\pi)^{-1} (\det C)^{-1/2} \exp \left[-\frac{1}{2} (C^{-1})_{\alpha\beta} \phi_{j,\alpha} \phi_{j,\beta} \right] d\phi_{j,\alpha'} \right) = \rho_G(\phi) \prod_{j=1}^N \prod_{\alpha'=1}^2 d\phi_{j,\alpha'}. \quad (2.17)$$

This measure should also be invariant under the deterministic nonlinear part of Eq. (2.8) with $A = 0$. There is some freedom in the discretization of nonlinearities. In our case, a natural constraint is to have the volume elements time-invariant, which is ensured by making the vector field divergence free, thereby leading to

$$\frac{d}{dt}\phi_{j,\alpha} = \frac{1}{3} G_{\beta\gamma}^{\alpha} \left(-\phi_{j-1,\beta} \phi_{j-1,\gamma} - \phi_{j-1,\beta} \phi_{j,\gamma} + \phi_{j,\beta} \phi_{j+1,\gamma} + \phi_{j+1,\beta} \phi_{j+1,\gamma} \right). \quad (2.18)$$

Then the time derivative of the action is

$$\begin{aligned} \frac{d}{dt} \log \rho_G &= -\frac{1}{3} \sum_{j=1}^N \phi_{j,\alpha} (C^{-1})_{\alpha\beta} G_{\gamma\gamma'}^{\beta} \\ &\quad \times \left(-\phi_{j-1,\gamma} \phi_{j-1,\gamma'} - \phi_{j-1,\gamma} \phi_{j,\gamma'} + \phi_{j,\gamma} \phi_{j+1,\gamma'} + \phi_{j+1,\gamma} \phi_{j+1,\gamma'} \right) \\ &= \frac{1}{3} \sum_{j=1}^N \left(\hat{G}_{\gamma\gamma'}^{\alpha} - \hat{G}_{\alpha\gamma'}^{\gamma} \right) (\phi_{j,\gamma} \phi_{j,\gamma'} \phi_{j+1,\alpha} - \phi_{j,\alpha} \phi_{j+1,\gamma} \phi_{j+1,\gamma'}). \end{aligned} \quad (2.19)$$

The sum vanishes only if the cyclicity condition (2.13) holds.

The cyclicity condition has been introduced in [9]. From the perspective of stochastic analysis, cyclicity of n -component stochastic Burgers equations is studied in [34, 36, 37].

2.4. Cyclic matrices

We assume that the fields have been linearly transformed such that $C = 1$. In view of Eq. (2.13), the matrices G^1 and G^2 are cyclic, if they are of the form

$$G^1 = \begin{pmatrix} a & b \\ b & c \end{pmatrix}, \quad G^2 = \begin{pmatrix} b & c \\ c & d \end{pmatrix} \quad (2.20)$$

with arbitrary coefficients a, b, c, d .

Since $C = 1$, it is natural to study how the dynamics behaves under orthogonal transformations of the fields. Reflection of either component yields the sign switches $(a, b, c, d) \rightarrow (a, -b, c, -d)$ and $(a, b, c, d) \rightarrow (-a, b, -c, d)$. Hence it suffices to consider the rotations given by

$$R = \begin{pmatrix} \cos \vartheta & \sin \vartheta \\ -\sin \vartheta & \cos \vartheta \end{pmatrix} \quad (2.21)$$

with $\vartheta \in [0, 2\pi]$, implying $R^T R = 1$. Setting

$$\tilde{\phi}_\alpha = R_{\alpha\beta} \phi_\beta, \quad (2.22)$$

the equations of motion

$$\partial_t \phi_\alpha - \partial_x (\langle \vec{\phi}, G^\alpha \vec{\phi} \rangle + D_{\alpha\beta} \partial_x \phi_\beta + B_{\alpha\beta} \xi_\beta) = 0 \quad (2.23)$$

from (2.8) with $A = 0$ transform to

$$\partial_t \tilde{\phi}_\alpha - \partial_x (\langle \tilde{\vec{\phi}}, \tilde{G}^\alpha \tilde{\vec{\phi}} \rangle + \tilde{D}_{\alpha\beta} \partial_x \tilde{\phi}_\beta + \tilde{B}_{\alpha\beta} \xi_\beta) = 0. \quad (2.24)$$

The transformed matrices are obtained as

$$\tilde{D} = R D R^T, \quad \tilde{B} = R B R^T, \quad \tilde{G}^\alpha = R_{\alpha\beta} R G^\beta R^T. \quad (2.25)$$

The matrices \tilde{D}, \tilde{B} are just another choice of D, B . In Appendix A we provide an explicit formula for \tilde{G}^α , from which one verifies that the transformed matrices \tilde{G}^1, \tilde{G}^2 satisfy again the cyclicity condition with $C = 1$. The transformed correlator is

$$\tilde{S}_{\alpha\beta}(x, t) = \langle \tilde{\phi}_\alpha(x, t) \tilde{\phi}_\beta(0, 0) \rangle. \quad (2.26)$$

Since the Gaussian measure with $C = 1$ is invariant under rotations, the correlator satisfies

$$\tilde{S}(x, t) = R S(x, t) R^T. \quad (2.27)$$

Thus the matrices $(\tilde{G}^1, \tilde{G}^2)$ are viewed as belonging to the same dynamical class as (G^1, G^2) .

2.5. Scaling hypothesis

As in the case of a single component, one argues that the transverse scale is $\xi_{\perp} \simeq t^{1/3}$ and the lateral scale $\xi_{\parallel} \simeq t^{2/3}$, see [38, 39]. Such property can be tested for specific observables. For the lateral scale, specifically we consider the spacetime correlator S of Eq. (2.14). For it the scaling assumption states

$$S(x, t) \simeq t^{-2/3} \mathbf{g}(t^{-2/3}x) \quad (2.28)$$

in approximation, for large x, t . The scaling function \mathbf{g} is a 2×2 matrix-valued function which, in principle, depends on all parameters of \vec{G} . According to the sum rule the normalization $\int dx \mathbf{g}_{\alpha\beta}(x) = \delta_{\alpha\beta}$ holds.

To monitor the transverse scale the most common choice is to consider step initial conditions, which however requires to solve the Riemann problem for the coupled deterministic Burgers equations, i.e. upon omitting noise and diffusion. An attempt in this direction is reported in [40]. The more accessible option is either flat, $\vec{\phi}(x) = 0$, or stationary initial conditions. The observable of interest is then the current across the origin integrated over the time interval $[0, t]$, denoted by $\vec{\mathcal{J}}_0(t)$. It has a leading deterministic term proportional to t and fluctuations on the transverse scale. Hence for large t ,

$$\vec{\mathcal{J}}_0(t) \simeq \vec{v}t + t^{1/3}\vec{\zeta}. \quad (2.29)$$

$\vec{\zeta}$ is a random 2-vector whose distribution depends, in principle, on all parameters of \vec{G} .

In case of a single component, clearly, at $\lambda = 0$ the scaling hypothesis fails and instead one will observe Gaussian fluctuations. Within the cyclicity class, assuming $C = 1$, the scaling hypothesis fails for the choices $(a, 0, 0, 0)$ and $(0, 0, 0, d)$ and their rotations. Using (A.2) and (A.3), in Dirac notation this leads to the exceptional coupling matrices

$$\begin{aligned} G^1 &= a \cos \vartheta | \cos \vartheta, -\sin \vartheta \rangle \langle \cos \vartheta, -\sin \vartheta |, \\ G^2 &= -a \sin \vartheta | \cos \vartheta, -\sin \vartheta \rangle \langle \cos \vartheta, -\sin \vartheta | \end{aligned} \quad (2.30)$$

and

$$\begin{aligned} G^1 &= d \sin \vartheta | \sin \vartheta, \cos \vartheta \rangle \langle \sin \vartheta, \cos \vartheta |, \\ G^2 &= d \cos \vartheta | \sin \vartheta, \cos \vartheta \rangle \langle \sin \vartheta, \cos \vartheta | \end{aligned} \quad (2.31)$$

for arbitrary $\vartheta \in [0, 2\pi]$. As to be discussed, the hypothesis holds for $(0, b, 0, 0)$ with $b \neq 0$ and $(0, 0, c, 0)$ with $c \neq 0$. As a general experience from non-degenerate flux Jacobians, further increasing the number of non-zero couplings does not change the scaling behavior. Thus it seems to be safe to conjecture that the two cases listed above are the only exceptional parameter values. Away from cyclicity, no clear picture is yet available. The immediate obstacle is the structure of the steady state. If the stationary measure has

a finite correlation length, then anticipated is the same dynamical behavior as for cyclic couplings.

2.6. Models to be studied

Since $C = 1$, no basis for the fields is singled out. One choice of a canonical basis for \vec{G} is then obtained through diagonalizing G^2 ,

$$G^1 = \begin{pmatrix} a & b \\ b & 0 \end{pmatrix}, \quad G^2 = \begin{pmatrix} b & 0 \\ 0 & d \end{pmatrix}. \quad (2.32)$$

In fact, for our numerical studies we will choose $a = 0$, so to be able to compare with the results of [14]. Thus

$$G^1 = b \begin{pmatrix} 0 & 1 \\ 1 & 0 \end{pmatrix}, \quad G^2 = b \begin{pmatrix} 1 & 0 \\ 0 & \lambda \end{pmatrix}, \quad (2.33)$$

where λ is regarded as a free parameter and b can be absorbed into a modified time scale.

The G_{11}^2 matrix element fixes the sign and hence $\lambda \in \mathbb{R}$. For $\lambda = 1$, the commutator $[G^1, G^2] = 0$ and through a rotation of $\pi/4$, the matrices are transformed to

$$\tilde{G}^1 = \sqrt{2}b \begin{pmatrix} 1 & 0 \\ 0 & 0 \end{pmatrix}, \quad \tilde{G}^2 = \sqrt{2}b \begin{pmatrix} 0 & 0 \\ 0 & 1 \end{pmatrix}. \quad (2.34)$$

Hence the system decouples into two one-component stochastic Burgers equations.

3. Numerical simulations of coupled stochastic Burgers and KPZ equations

For the numerical studies, we focus on the model defined by the matrices G^1, G^2 of Eq. (2.33). Hence the Langevin equations are

$$\begin{aligned} \partial_t \phi_1 &= \partial_x (\partial_x \phi_1 + 2b\phi_1\phi_2 + \sqrt{2}\xi_1), \\ \partial_t \phi_2 &= \partial_x (\partial_x \phi_2 + b(\phi_1^2 + \lambda\phi_2^2) + \sqrt{2}\xi_2). \end{aligned} \quad (3.1)$$

In our simulations, diffusion is fixed to 1 and noise strength to $\sqrt{2}$, so that the static covariance equals $C = 1$. The initial data are random and given by the Gaussian measure (2.17) with $C = 1$. For $\lambda = 1$, after a rotation by $\pi/4$, the system decouples into two independent stochastic Burgers equations. For our numerical simulations we focus on the case $\lambda = 0$. For a non-degenerate Jacobian, only by setting some coefficients to 0 a distinct universality can be accomplished. Thus $\lambda = 0$ has a good chance for exhibiting a non-KPZ behavior. We perform direct numerical simulations (DNSs) of Eq. (3.1) using the discretization scheme provided in Eqs. (2.16), (2.18). Of interest is the spacetime

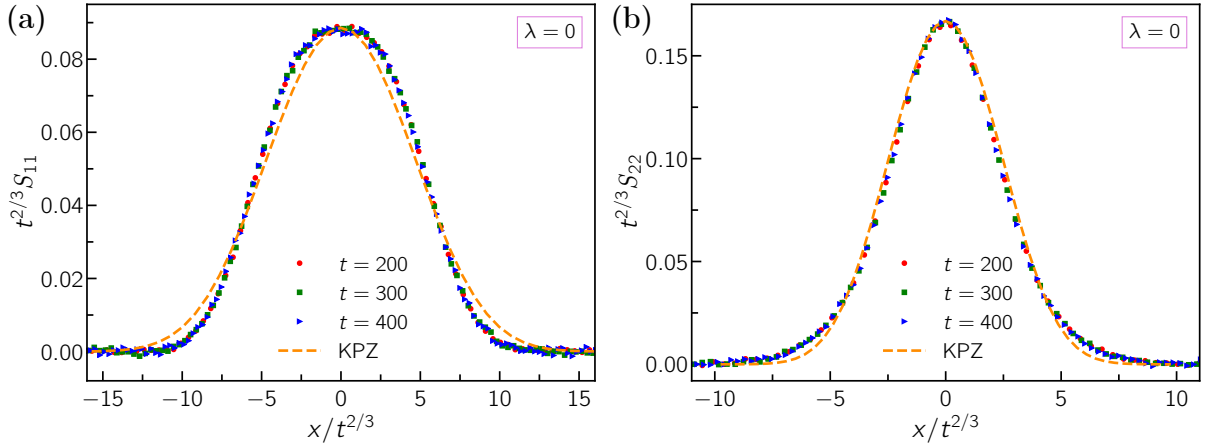


Figure 1: Correlators S_{11} and S_{22} obtained from numerical simulations of the coupled stochastic Burgers equations in Eq. (3.1) with $b = 3$ and $\lambda = 0$ using the discretizations of Eqs. (2.16) and (2.18). The system size is $L = 4096$ and the number of independent simulations is 10^5 . The covariance of the initial correlator is $\langle \phi_{\alpha,j} \phi_{\beta,0} \rangle = \delta_{\alpha\beta} \delta_{j0}$. The sum rule, $\sum_j S_{11}(j, t) = \sum_j S_{22}(j, t) = 1$, is satisfied within a numerical accuracy of 1%.

correlator $S_{\alpha\beta}$ as defined in Eq. (2.14). The Gaussian measure is invariant under the change $\phi_1 \rightsquigarrow -\phi_1$. Invariance of Eq. (3.1) under this transformation implies that $\phi_1(x, t)$ has an even distribution. From this property one concludes that $S_{12}(x, t) = 0 = S_{21}(x, t)$, which is very well satisfied numerically.

The real task is to compute S_{11} and S_{22} for $\lambda = 0$. Our results are displayed in Fig. 1 and, considering the full time sequence (not plotted), it appears that the numerical results are already in the scaling regime. First of all, one notes that the anticipated $t^{\frac{2}{3}}$ scaling exponent is very well satisfied. At $\lambda = 1$, the system is decoupled and S_{11} , S_{22} would scale with f_{KPZ} having the same value for coefficient Γ_{\parallel} . At $\lambda = 0$ one observes that S_{11} is bulky and S_{22} slim. More importantly they differ from f_{KPZ} . Even allowing for linear scale change with a single parameter Λ , S_{11} differs significantly from S_{22} . Thus as, a so far preliminary, conclusion: the scaling exponent conforms with the one-component model, but the scaling function depends on the coupling λ not merely through a single non-universal time scale coefficient Γ_{\parallel} .

The second task concerns the time integrated currents. By Eq. (3.1) the instantaneous currents are defined as

$$\mathcal{J}_1 = -(\partial_x \phi_1 + 2b\phi_1\phi_2 + \sqrt{2}\xi_1), \quad \mathcal{J}_2 = -(\partial_x \phi_2 + b(\phi_1^2 + \lambda\phi_2^2) + \sqrt{2}\xi_2). \quad (3.2)$$

Numerically, it is convenient to switch to the height field through

$$\partial_x h_\alpha = \phi_\alpha. \quad (3.3)$$

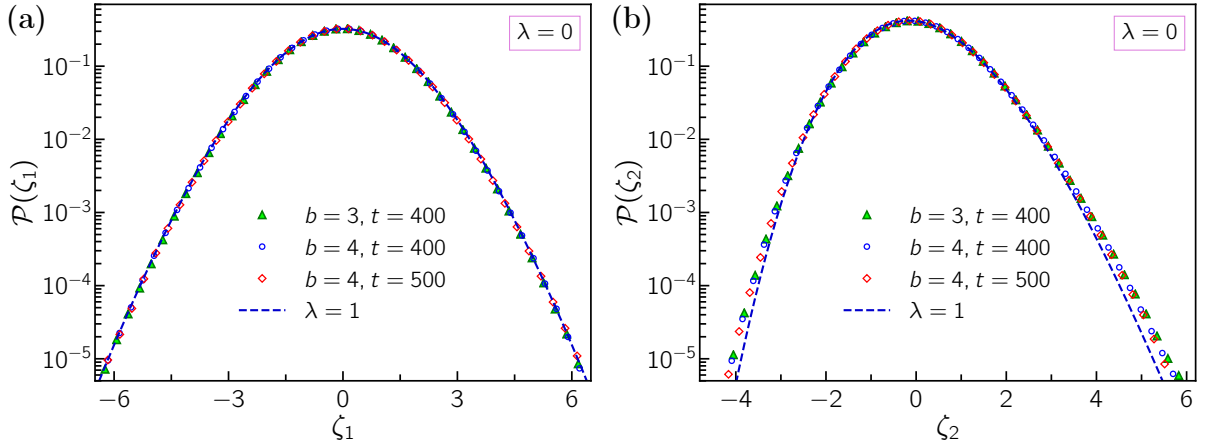


Figure 2: Probability density functions (PDFs) of (a) ζ_1 and (b) ζ_2 for the coupled KPZ equations (3.4) at $\lambda = 0$ for different values of the parameter b and a sequence of times t . The system size is $L = 8192$ with periodic boundary conditions. The total number of simulation runs is 5×10^4 . For both ζ_1 and ζ_2 we set $\Gamma_\perp = b$. The corresponding PDFs collapse on a single curve. The variances for ζ_1 and ζ_2 are 1.545 and 0.943, respectively. Comparison is with the corresponding quantities at $\lambda = 1$.

The Langevin equations for the KPZ height fields h_α are then

$$\begin{aligned}\partial_t h_1 &= \partial_{xx} h_1 + 2b \partial_x h_1 \partial_x h_2 + \sqrt{2} \xi_1, \\ \partial_t h_2 &= \partial_{xx} h_2 + b \left((\partial_x h_1)^2 + \lambda (\partial_x h_2)^2 \right) + \sqrt{2} \xi_2.\end{aligned}\tag{3.4}$$

Because of the conservation law, height fields and currents are related as

$$h_\alpha(x, t) - h_\alpha(x, 0) = - \int_0^t ds \mathcal{J}_\alpha(x, s),\tag{3.5}$$

where $\mathcal{J}_\alpha(x, s)$ is the instantaneous current (3.2) evaluated at (x, s) . For the simulations, space is discretized with index $0, \dots, L - 1$ and the height satisfies helical boundary conditions. In our set up, the initial height field has independent unit Gaussian zero mean increments and helical constraint becomes $h_L = h_0$. At large times, to leading order the height fields increase linearly in t ,

$$h_\alpha(t) \simeq v_\alpha t.\tag{3.6}$$

For the discretization according to Eqs. (2.16), (2.18) the velocity is given by

$$v_\alpha = \frac{2}{3} G_{\gamma\gamma}^\alpha,\tag{3.7}$$

as well confirmed numerically. To study the fluctuations, the linear term is subtracted leading to

$$\zeta_\alpha = \Gamma_\perp^{-\frac{1}{3}} t^{-1/3} (h_\alpha(x, t) - h_\alpha(0) - v_\alpha t), \quad (3.8)$$

where for notational simplicity we introduced already the scale factor $\Gamma_\perp^{-\frac{1}{3}}$.

In Fig. 2, we confirm that ζ_α has a well-defined limiting distribution, independent of x by stationarity. By definition $\vec{\zeta}$ is a random vector, which has a two-dimensional distribution. Numerically determined are only the two marginals. In Fig. 2 we display the PDFs of ζ_1 and ζ_2 at $\lambda = 0$ and compare with the corresponding PDFs at $\lambda = 1$. Note that at $\lambda = 1$, after a rotation by $\pi/4$, the resulting vector $(\zeta_+, \zeta_-) = (1/\sqrt{2})(\zeta_1 + \zeta_2, -\zeta_1 + \zeta_2)$ has independent components, both Baik-Rains distributed [41]. Hence in Fig. 2 we compare with sum and differences of two independent Baik-Rains PDFs. As we decrease λ , independence is lost and the probability density functions of the two marginals appear to differ significantly from the one of Baik-Rains. Note that ζ_- is symmetric but distinct from a Gaussian.

Distribution	M	V	\$	K
Baik-Rains [41, 42]	0	1.150	0.359	0.289
ζ_1	0	1.545	0	0.152
ζ_2	-0.025	0.943	0.250	0.236
$(\zeta_1 + \zeta_2) / \sqrt{2}$	-0.018	1.243	0.307	0.253
$(-\zeta_1 + \zeta_2) / \sqrt{2}$	-0.017	1.245	0.307	0.256

Table 1: Comparing skewness \$ and excess kurtosis K of the Baik-Rains distribution with the ones for ζ_1 and ζ_2 . These values are obtained by averaging over the time interval [425, 500] for $b = 4$ and $L = 8192$. By stationarity, the means of ζ_α equal 0. The last two rows display the values for symmetric and antisymmetric combinations of ζ_1 and ζ_2 , see also Appendix C.

For a more quantitative comparison, the dimensionless form of skewness, \$, and kurtosis, K is listed in Table 1, where for some random variable, X , with mean M and

variance \mathbb{V} , skewness and kurtosis are defined through

$$\mathbb{M} = \langle X \rangle, \quad \mathbb{V} = \langle (X - \mathbb{M})^2 \rangle, \quad \mathbb{S} = \mathbb{V}^{-3/2} \langle (X - \mathbb{M})^3 \rangle, \quad \mathbb{K} = \mathbb{V}^{-2} \langle (X - \mathbb{M})^4 \rangle - 3. \quad (3.9)$$

We also added the values for $(\pm\zeta_1 + \zeta_2)/\sqrt{2}$ (see [Appendix C](#)). ζ_1 and ζ_2 are not independent and the sum is performed for each realization. As to be noted, in terms of skewness and kurtosis, ζ_1 differs significantly from Baik-Rains, while ζ_2 is still different, but somewhat less so.

4. Two-lane lattice gas

For one component, KPZ universality is confirmed not only for the continuum equation, but also for discrete models as TASEP and ASEP. Such results strongly support the KPZ scaling theory which asserts the lateral time scale $t^{\frac{2}{3}}$, the transversal time scale $t^{\frac{1}{3}}$, universal scaling functions, and corresponding non-universal coefficients. Up to constants independent of λ , the latter are given by $\Gamma_{\parallel} = 2|\lambda|\sqrt{2\chi}$ and $\Gamma_{\perp} = |\lambda|\chi^2$, where $\lambda = j''(\rho)/2$ with $j(\rho)$ the average current. Examples of two-component systems with a non-degenerate flux Jacobian are the Arndt-Heinzel-Rittenberg (AHR) [[43](#), [44](#), [18](#)] and the Bernardin-Stoltz (BS) [[45](#), [46](#)] models. The predictions based on nonlinear fluctuating hydrodynamics [[47](#), [9](#)] have been well confirmed in [[18](#)] and [[46](#)], but do not cover the degenerate case.

The first task is to find a suitable lattice gas model. Our search has been guided by possessing a product invariant stationary measure and a minimal number of states at each lattice site. The AHR model has three local states, $(-,0,+)$. For its stationary measures the matrix product construction is required [[18](#)]. As it turns out, the flux Jacobian is non-degenerate over the entire parameter range. Popkov and Schütz studied two-lane models with local states $(00,01,10,11)$. The version studied in [[30](#)] satisfies our conditions, but the flux Jacobian is again non-degenerate. An earlier variant can be found in [[6](#)]. This two-lane model allows for degeneracy, as investigated in [[48](#)] under the label “umbilic point”. The flux Jacobian is still explicit. Hence this stochastic two-lane lattice gas is optimally qualified for our purposes.

The basic elements of the KPZ scaling theory are easily generalized. The lattice gas has two conserved densities. The steady states are labelled by the average densities $\vec{\rho}$. For our model the average currents, $\vec{j}(\vec{\rho})$, are given and hence also the flux Jacobian. (G^1, G^2) are the matrices of second derivatives for $j_1(\vec{\rho}), j_2(\vec{\rho})$. The unique point of degeneracy turns out to be density $1/2$ in each lane. To compare with Eq. ([3.1](#)), the crucial insight is to first match the static susceptibility. For the continuum equation we adopted the convention $C = 1$. Thus for the lattice gas we have to diagonalize C and then rescale so to achieve a unit matrix. This linear transformation has to be applied to

(G^1, G^2) , as already discussed in Section 2. The transformed matrices then appear in the approximation through a stochastic continuum equation.

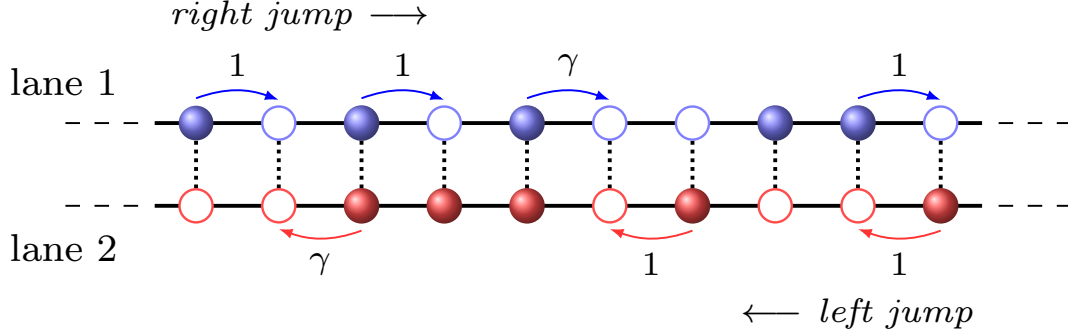


Figure 3: Illustrating the two-lane lattice gas model [48]. The lattice sites are indexed by (α, n) where $\alpha = 1, 2$, $n \in \mathbb{Z}$.

In the two-lane model of Popkov and Schütz, the sites are labeled by (α, n) , $\alpha = 1, 2$, $n \in \mathbb{Z}$. The occupation variables are $\eta_{\alpha, n}$ with values 0, 1, where $\alpha = 1$ is also referred to as top lane and $\alpha = 2$ as bottom lane, see Fig. 3. Under the exclusion rule, particles in lane 1 jump only to the right and in lane 2 only to the left. The jump rates, equivalently exchange rates, are given by

$$\begin{aligned} W_{n, n+1}^1 &= \eta_{1, n}(1 - \eta_{1, n+1}) + (\gamma - 1)\eta_{1, n}(1 - \eta_{1, n+1})\eta_{2, n}(1 - \eta_{2, n+1}), \\ W_{n, n+1}^2 &= (1 - \eta_{2, n})\eta_{2, n+1} + (\gamma - 1)(1 - \eta_{2, n})\eta_{2, n+1}(1 - \eta_{1, n})\eta_{1, n+1} \end{aligned} \quad (4.1)$$

with $\gamma > 0$. Particles stay in their own lane. If $\gamma = 1$, then lane 1 is TASEP with jumps of rate 1 to the right and lane 2 is TASEP with jumps of rate 1 to the left. The interaction between lanes results from varying γ . If in lane 1 at sites $n, n + 1$ the configuration is 10, then at sites $n, n + 1$ in lane 2 the possible configurations are 00, 10, 01, 11. In case 10 shows, the jump rate in lane 1 is modified to γ , while in the three other cases the jump rate stays to be equal to 1. If in lane 2 at sites $n, n + 1$ the configuration is 01, the jump rates are given by the corresponding mirror image, see Fig. 3.

As established in [6], the invariant measures are product with respect to n . To study their properties it thus suffices to consider a single site. For lighter notation we set $\eta_{1, 0} = \vartheta$ and $\eta_{2, 0} = \theta$. Then the possible states are 00, 10, 01, 11 and the single site measure of the steady state is

$$p_{\vartheta\theta} = \frac{1}{Z} \exp\left(-2\nu\vartheta\theta + \mu\vartheta + \tilde{\mu}\theta\right). \quad (4.2)$$

Here $\gamma = e^{2\nu}$, $\mu, \tilde{\mu}$ are chemical potentials, and Z is normalizing partition function. (Note

that our 2ν equals ν of [48]). Setting $p_{11} = \Omega$, one obtains

$$\Omega = \frac{1}{2q} \left(-1 - q(1 - u - v) + \sqrt{(1 + q(1 - u - v))^2 + 4quv} \right) \quad (4.3)$$

with

$$q = \gamma - 1, \quad u = \langle \vartheta \rangle, \quad v = \langle \theta \rangle. \quad (4.4)$$

The particle density on the top-lane is u and the one on the bottom-lane v . Then

$$p_{00} = 1 - u - v + \Omega, \quad p_{01} = v - \Omega, \quad p_{10} = u - \Omega, \quad p_{11} = \Omega. \quad (4.5)$$

The static covariance matrix is given by

$$C_{\alpha\beta}(u, v) = \langle \eta_{\alpha,0} \eta_{\beta,0} \rangle - \langle \eta_{\alpha,0} \rangle \langle \eta_{\beta,0} \rangle, \quad C(u, v) = \begin{pmatrix} u(1-u) & \Omega - uv \\ \Omega - uv & v(1-v) \end{pmatrix}. \quad (4.6)$$

The average currents have been computed in [6, 48] with the result

$$j_1(u, v) = u(1-u) + q\Omega(1-u-v+\Omega), \quad j_2(u, v) = -v(1-v) - q\Omega(1-u-v+\Omega). \quad (4.7)$$

From Eq. (4.7) one deduces the flux Jacobian

$$A = \begin{pmatrix} 1-2u & 0 \\ 0 & -1+2v \end{pmatrix} + q\Omega \begin{pmatrix} -1 & -1 \\ 1 & 1 \end{pmatrix} + q((1-u-v) + 2\Omega) \begin{pmatrix} \partial_u \Omega & \partial_v \Omega \\ -\partial_u \Omega & -\partial_v \Omega \end{pmatrix}. \quad (4.8)$$

For $q = 0$, the line of degeneracy equals $\{1 - u - v = 0\}$. As proved in the Appendix, for $q > -1$, $q \neq 0$, the only point of degeneracy in the interior of the square $[0, 1]^2$ is $u = \frac{1}{2} = v$, in which case both eigenvalues are 0. Then the covariance simplifies to

$$C(\frac{1}{2}, \frac{1}{2}) = C = \frac{1}{4} \begin{pmatrix} 1 & -1 \\ -1 & 1 \end{pmatrix} + \Omega \begin{pmatrix} 0 & 1 \\ 1 & 0 \end{pmatrix}, \quad (4.9)$$

which has eigenvalues

$$\lambda_1^2 = \Omega(\frac{1}{2}, \frac{1}{2}) = \frac{1}{2(1+e^\nu)}, \quad \lambda_2^2 = \frac{1}{2} - \Omega(\frac{1}{2}, \frac{1}{2}) = \frac{1}{2(1+e^{-\nu})}. \quad (4.10)$$

The average currents turn out to be given by

$$j_1(\frac{1}{2}, \frac{1}{2}) = \frac{1}{2(1+e^{-\nu})}, \quad j_2(\frac{1}{2}, \frac{1}{2}) = -j_1(\frac{1}{2}, \frac{1}{2}). \quad (4.11)$$

To relate the lattice gas with the continuum Burgers equation in (2.8), we follow the strategy laid out in nonlinear fluctuating hydrodynamics. The currents (4.7) determine the Euler equations of the two-lane model, which can be written as

$$\partial_t u + \partial_x j_1(u, v) = 0, \quad \partial_t v + \partial_x j_2(u, v) = 0. \quad (4.12)$$

The background state has constant densities $\frac{1}{2}$. Thus we expand the currents j_1, j_2 as $u = \frac{1}{2} + u_1, v = \frac{1}{2} + u_2$. The linear term is the flux Jacobian evaluated at $u = \frac{1}{2} = v$. This term vanishes, thereby confirming that in the steady state there is no ballistic component. To second order in u_1, u_2 one obtains

$$\begin{aligned} j_1\left(\frac{1}{2} + u_1, \frac{1}{2} + u_2\right) &= j_1\left(\frac{1}{2}, \frac{1}{2}\right) + \frac{1}{2}\langle \vec{u}, H^1 \vec{u} \rangle, \\ j_2\left(\frac{1}{2} + u_1, \frac{1}{2} + u_2\right) &= -j_1\left(\frac{1}{2}, \frac{1}{2}\right) + \frac{1}{2}\langle \vec{u}, H^2 \vec{u} \rangle. \end{aligned} \quad (4.13)$$

Here the second order matrices are

$$H^1 = \begin{pmatrix} -1 & 0 \\ 0 & 0 \end{pmatrix} - H^\diamond, \quad H^2 = \begin{pmatrix} 0 & 0 \\ 0 & 1 \end{pmatrix} + H^\diamond \quad (4.14)$$

with

$$H^\diamond = \frac{1}{2} \begin{pmatrix} \sinh \nu & \cosh \nu - 1 \\ \cosh \nu - 1 & \sinh \nu \end{pmatrix}. \quad (4.15)$$

Recalling the discussion in Section 2, a comparison with the continuum equations requires to transform the static covariance C to the identity matrix. This is done in the two steps $\tilde{u}_\alpha = R_{\alpha\beta} u_\beta$ and $\varphi_\alpha = (Q^{-1})_{\alpha\beta} \tilde{u}_\beta$, where R represents rotation by $\pi/4$,

$$R = \frac{1}{\sqrt{2}} \begin{pmatrix} 1 & 1 \\ -1 & 1 \end{pmatrix}, \quad (4.16)$$

and Q is the diagonal matrix

$$Q = \begin{pmatrix} \lambda_1 & 0 \\ 0 & \lambda_2 \end{pmatrix}. \quad (4.17)$$

Hence C is transformed as

$$Q^{-1} R C R^T Q^{-1} = 1. \quad (4.18)$$

Applying the rotation to H^α yields

$$2RH^1R^T = \begin{pmatrix} -1 & 1 \\ 1 & -1 \end{pmatrix} - \begin{pmatrix} e^\nu - 1 & 0 \\ 0 & 1 - e^{-\nu} \end{pmatrix} \quad (4.19)$$

and

$$2RH^2R^T = \begin{pmatrix} 1 & 1 \\ 1 & 1 \end{pmatrix} + \begin{pmatrix} e^\nu - 1 & 0 \\ 0 & 1 - e^{-\nu} \end{pmatrix}. \quad (4.20)$$

Using $\tilde{H}^\alpha = R_{\alpha\beta} R H^\beta R^T$, valid for orthogonal transformations, one arrives at

$$\tilde{H}^1 = \frac{1}{\sqrt{2}} \begin{pmatrix} 0 & 1 \\ 1 & 0 \end{pmatrix}, \quad \tilde{H}^2 = \frac{1}{\sqrt{2}} \begin{pmatrix} e^\nu & 0 \\ 0 & 2 - e^{-\nu} \end{pmatrix}. \quad (4.21)$$

In the second step \tilde{H}^α is transformed under Q^{-1} . We denote the transformed matrices by G^α , since they appear in the continuum approximation (2.8) with $A = 0$ and $C = 1$, i.e. $D + D^T = BB^T$. In formulas, because $Q = Q^T > 0$, one has $G^\alpha = (Q^{-1})_{\alpha\beta} Q \tilde{H}^\beta Q$ and hence

$$G^1 = b \begin{pmatrix} 0 & 1 \\ 1 & 0 \end{pmatrix}, \quad G^2 = b \begin{pmatrix} 1 & 0 \\ 0 & 2 - \frac{1}{\sqrt{\gamma}} \end{pmatrix}, \quad b = \frac{1}{2\sqrt{2}} \lambda_2. \quad (4.22)$$

The extra factor of $1/2$ in the definition of b results from the Taylor expansion in (4.13). Evidently \vec{G} is cyclic. In Eq. (4.22) the parameter b is merely a time scale. Multiplying all jump rates with a constant factor would modify the parameter b . More important is the relation

$$\lambda = 2 - \frac{1}{\sqrt{\gamma}}, \quad (4.23)$$

which determines the parameter of the stochastic Burgers equation at which its asymptotic behavior coincides with the one of the lattice gas.

Since $\gamma > 0$, the range of λ is $[-\infty, 2]$, $\lambda = 0$ corresponding to $\gamma = 0.25$. The lattice gas cannot reach values of λ beyond 2. At $\gamma = \infty$, the lattice gas is still well defined, only some specific exchanges occur instantaneously. Surprisingly, also negative values of λ show up. Note that the sign of λ cannot be trivially removed due to $b^{-1} G_{11}^2 = 1$. For small γ , there are many almost blocked configurations and the current vanishes as $\sqrt{\gamma}$. This indicates that the convergence to the scaling regime will be very slow.

These results could not have been anticipated. The strategy employed is general, but the fact that the two-lane model turns out to have cyclic \vec{G} matrices is specific. Nonlinear fluctuation theory predicts that on large scales the two-lane model and the stochastic Burgers equation (3.1) with $\lambda = 2 - 1/\sqrt{\gamma}$ and $b = \lambda_2/2\sqrt{2}$ have the same scaling behavior, provided the fields are properly transformed. A numerical check will be discussed in Section 6. In the case of a non-degenerate flux Jacobian, according to nonlinear fluctuating hydrodynamics the correctly adjusted fields are the eigenmodes of A . In the degenerate case these turn trivial and instead the covariance matrix C plays a central role.

5. Numerical simulations of the two-lane lattice gas

The two-lane model is considered on a ring of L sites, to say $n = 0, \dots, L - 1$, with periodic boundary conditions. The initial data are random: at each site independently the distribution (4.2) is generated with chemical potentials $\mu = \tilde{\mu} = (\log \gamma)/2$ corresponding to density $1/2$. Rather than a whole range of γ 's, we choose only $\gamma = 0.25$, which corresponds to $\lambda = 0$ and is maximally away from the decoupled $\gamma = 1$. For the dynamics a standard Monte Carlo scheme is used, as described in [48]. System size is $L = 2^{16}$

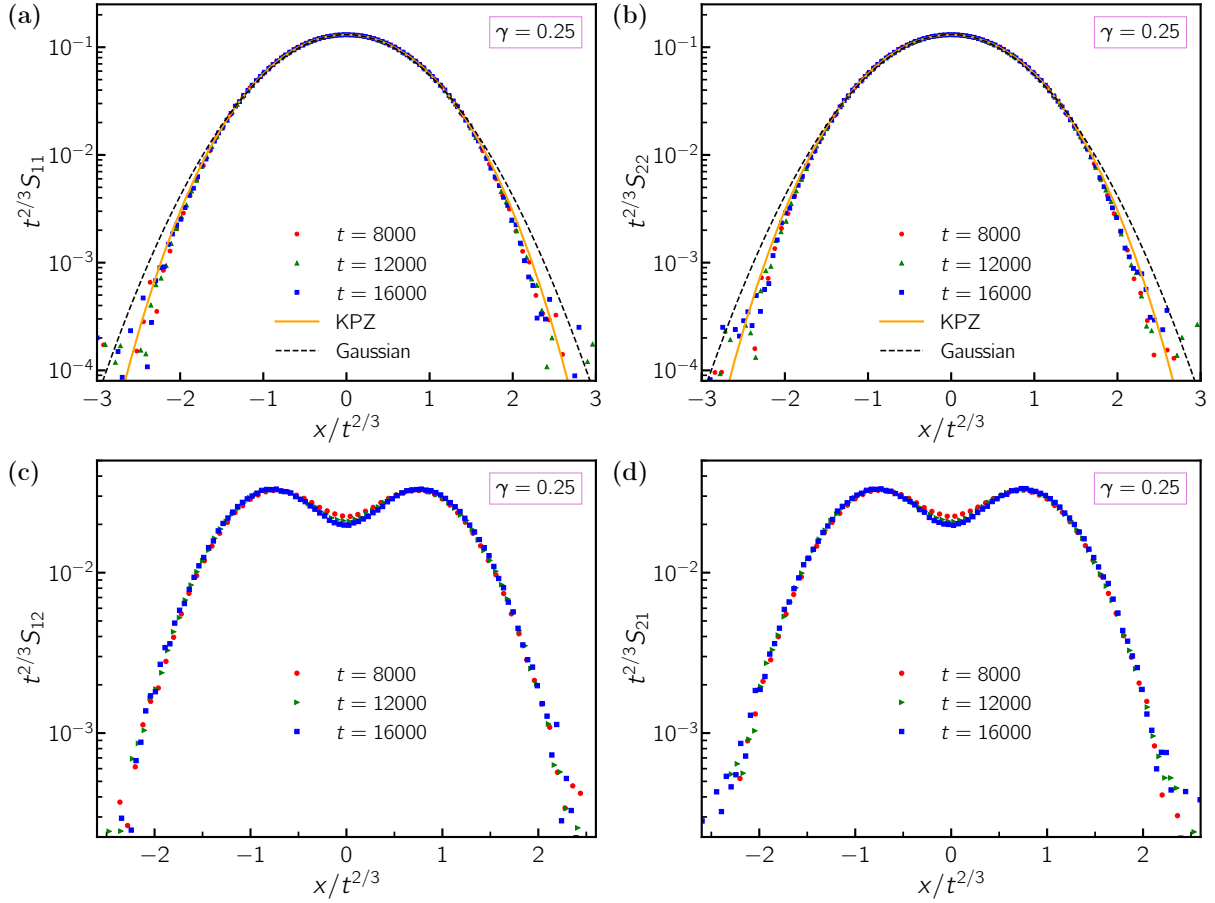


Figure 4: Plots of the correlator $\mathcal{S}_{\alpha\beta}$ for the two lanes in the lattice-gas model with $\gamma = 0.25$. The system size is $L = 2^{16}$ and the number of independent simulations is 4×10^5 . The initial measure is provided in Eq. (4.2) with $\mu = \tilde{\mu} = (\log \gamma)/2$ corresponding to the density $1/2$ in each of the lanes. In accordance with the sum rule, within a numerical accuracy of 1%, $\sum_n \mathcal{S}_{11}(n, t) = 1/4$ and $\sum_n \mathcal{S}_{12}(n, t) = 1/12$, where $1/4, 1/12$ is the value at $t = 0$.

and simulation time is up to MC 20000 time steps where a MC time step is $2L$ random sequential updates. Recorded is the spacetime correlation matrix

$$\mathcal{S}_{\alpha\beta}(n, t) = \left\langle (\eta_{\alpha,n}(t) - \frac{1}{2})(\eta_{\beta,0}(0) - \frac{1}{2}) \right\rangle. \quad (5.1)$$

Numerically the bracket $\langle \cdot \rangle$ is an average over realizations and lattice points. Due to the conservation law the sum rule

$$\sum_{n=0}^{L-1} \mathcal{S}(n, t) = C \quad (5.2)$$

holds. Exchanging particles and holes is equivalent to exchanging lanes 1 and 2. Therefore

$$S_{11}(n, t) = S_{22}(n, t), \quad S_{12}(n, t) = S_{21}(n, t). \quad (5.3)$$

Thus only S_{11} and S_{12} have to be measured. Our results are displayed in Fig. 4, which includes S_{22} and S_{21} as control check.

The anticipated scaling with the power law $2/3$ is very well confirmed. The sum rule (5.2) holds with high precision. At $\gamma = 1$, one has two independent TASEPs and cross correlations vanish. When tuning to $\gamma = 0.25$, S_{12} is nonzero and develops a local minimum at $n = 0$. The correlator matrix has changed dramatically. Accidentally, S_{11} is rather close to f_{KPZ} . These results convincingly establish that the correlator S continuously deforms by varying γ . There is no evidence that the structure of this 2×2 matrix is related to the single component case.

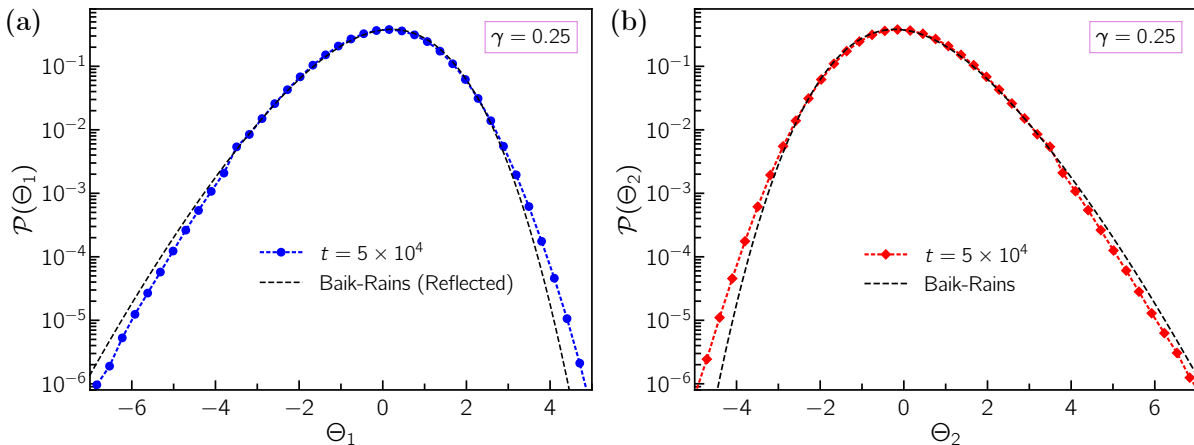


Figure 5: Plots of PDFs for Θ_1 and Θ_2 in the two-lane lattice gas model for $\gamma = 0.25$. The initial configurations are chosen from the stationary measure (4.2) at exact half-filling in each lane. (a) is a mirror image of (b).

The other observable of interest is the α -current, $J_{\alpha,n}(t)$, across the bond $(n, n + 1)$ integrated over the time span $[0, t]$. This simply amounts to count the number of exchanges at the bond $(n, n + 1)$ in lane α up to time t . By particle-hole symmetry, in distribution,

$$J_{2,n}(t) = -J_{1,n}(t). \quad (5.4)$$

Employing a law of large numbers $J_{\alpha,0}(t) \simeq j_\alpha t$ with $j_1 = \gamma^{1/2}/2(1 + \gamma^{1/2})$, $j_2 = -j_1$, according to Eq. (4.11). As discussed before, the integrated current fluctuations are expected to be of order $t^{1/3}$. Hence one studies the limit of large t as

$$\lim_{t \rightarrow \infty} t^{-1/3}(J_{\alpha,0}(t) - j_\alpha t) = \Theta_\alpha, \quad (5.5)$$

where Θ_α is still random.

As displayed in Fig. 5, at least numerically a limiting random distribution is established. For $\gamma = 1$, the limit Θ_1 is known to be the Baik-Rains distribution. Our simulation confirms this fact with good precision. On the other hand, for $\gamma = 0.25$, while the distribution looks qualitatively similar, they are clearly distinct. Quantitatively, for $\gamma = 0.25$ skewness equals 0.278 and kurtosis 0.237, which should be compared with the Baik-Rains values of 0.359 and 0.289. This result further supports our scenario of continuous deformation as changing γ . Particle-hole symmetry implies $\Theta_1 = -\Theta_2$ in distribution, which is well confirmed.

6. Universality

Having numerical data for continuum and discrete models offers the possibility to check for KPZ universality. The parameter correspondence of the two models is given by

$$\lambda = 2 - \frac{1}{\sqrt{\gamma}}, \quad b = \frac{1}{2\sqrt{2}}\lambda_2, \quad (6.1)$$

compare with (4.22). For a single component, KPZ scaling theory separates into model-dependent parameters and universal scaling functions. For our case, no such theory is available, but some aspects can be tested. Following the steps in Section 4, it is natural to introduce the random field

$$\varphi_{\alpha,n} = (Q^{-1}R)_{\alpha\beta}(\eta_{\beta,n} - \frac{1}{2}). \quad (6.2)$$

Then, in our context of time stationary initial conditions, KPZ universality means that the statistics of $\varphi_{\alpha,n}(t)$ is close to the statistics of the field $\phi_\alpha(x, t)$, as governed by the stochastic Burgers equation (3.1). More precisely, long time scaling functions are identical up to model-dependent parameters.

Our first test concerns the spacetime correlator of $\varphi_{\alpha,n}(t)$ at $\gamma = 0.25$, which according to Eq. (5.1) is given by

$$Q^{-1}RS(n, t)R^TQ^{-1} = P(n, t). \quad (6.3)$$

Its 12 matrix element is very close to zero. The matrix elements $P_{11}(n, t)$, $P_{22}(n, t)$ are now compared with $S_{11}(x, t)$, $S_{22}(x, t)$, which have been reported already in Section 3. Their asymptotics scales with b . Thus we pick $b = 3$ as standard and simply replot the two correlators in Fig. 6. For the matrix element $P_{11}(n, t)$, we consider the longest available time and set up an area preserving one-parameter fit defined by

$$(at)^{\frac{2}{3}}P_{11}\left((at)^{2/3}y, t\right), \quad (6.4)$$

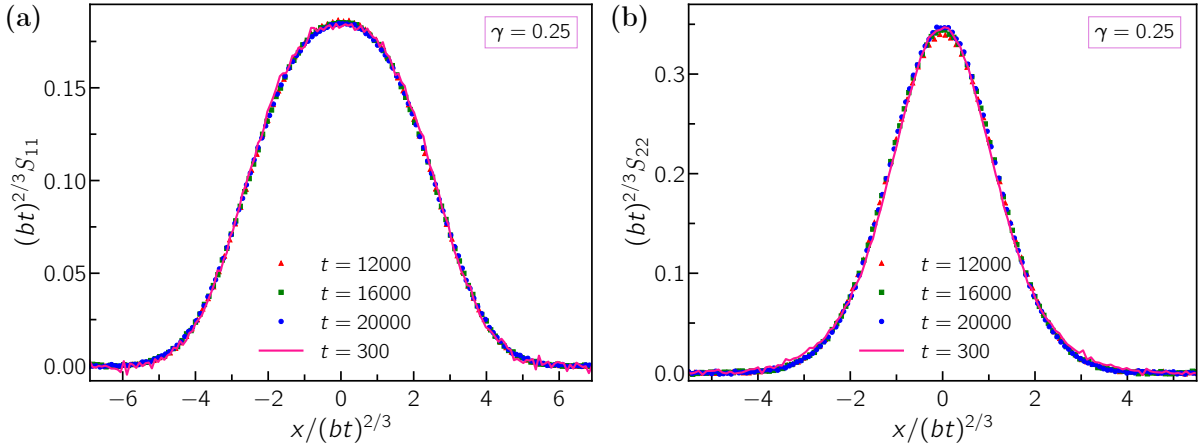


Figure 6: Comparison of the spacetime correlators (a) S_{11} with P_{11} and (b) S_{22} with P_{22} . The solid lines in deep pink represent the spacetime correlators, S_{11} and S_{22} , of the coupled stochastic Burgers equations at $\lambda = 0, b = 3$. The red, green, and blue filled symbols represent the correlators, P_{11} and P_{22} , for the two-lane model at $\gamma = 0.25$.

where $y = n/(at)^{2/3}$ is of order 1. The parameter a is varied to optimize the agreement with the given $S_{11}(x, t)$ and the optimal a is denoted by $\Lambda_{\parallel,1}$. In fact it suffices to compare the maxima. Other notions would lead essentially to the same result. Correspondingly we handle $P_{22}(n, t)$ with a distinct optimal parameter $\Lambda_{\parallel,2}$. As confirmed by Fig. 6 this fit works unambiguously. Taking the “wrong” value of γ or a different linear transformation, the one-parameter fit would fail. The numerical values at $t = 20000$ are $\Lambda_{\parallel,1} = 0.26$ and $\Lambda_{\parallel,2} = 0.37$.

The second test refers to the time-integrated currents as in (5.5). According to the rules the transformed random current is

$$t^{-\frac{1}{3}}(Q^{-1}R)_{\alpha\beta}(J_{\beta,0}(t) - j_{\beta}t) = \Xi_{\alpha}(t). \quad (6.5)$$

The free parameter a is inserted in the PDF at longest time as

$$a^{-\frac{1}{3}}\Xi_{\alpha}(t), \quad (6.6)$$

$\alpha = 1, 2$. The parameter a is optimized such that the PDF agrees maximally with the reference standard, which is the PDF plotted in Fig. 2 with $b = 4$. The optimal a is denoted by $\Lambda_{\perp,\alpha}$. In fact, as before, it suffices to compare the maxima of the PDFs. The result is displayed in Fig. 7. The numerical values are $\Lambda_{\perp,1} = 2.18$ and $\Lambda_{\perp,2} = 2.74$.

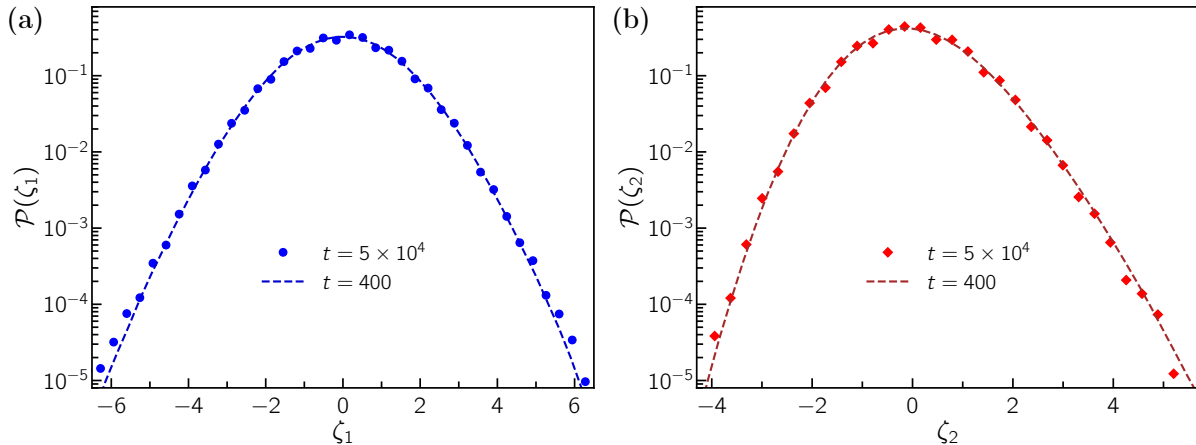


Figure 7: Comparison of the PDFs of fluctuations of the time-integrated current (a) ζ_1 with Ξ_1 and (b) ζ_2 with Ξ_2 . The dashed lines represent the PDFs for the coupled stochastic Burgers equations at $\lambda = 0$, $b = 4$. The filled symbols represent the data for the two-lane model at $\gamma = 0.25$.

Giving that only a single parameter is adjusted, for both tests the fit is surprisingly accurate. For our particular choice of parameters, universality is well confirmed. The numerically obtained scaling functions differ from those known for the one-component system. In this case, KPZ scaling theory fixes the value of Λ_{\parallel} and Λ_{\perp} . It would be of interest to better understand their origin in our context.

7. Mode-coupling theory

Mode-coupling theory is a self-consistent one-loop approximation for the correlator S of Eq. (2.14), see [49]. With fair success it has been applied to multi-component KPZ equations in the non-degenerate setting [9]. Thus it is of interest to understand the predictions of this theory for a model with a degenerate flux Jacobian. The derivation of the mode-coupling equations is discussed in [9]. They have to be specialized to a vanishing linear flux term.

Mode-coupling approximation is usually written in Fourier space for

$$\hat{S}(k, t) = \sum_{j \in \mathbb{Z}} e^{ikj} S(j, t). \quad (7.1)$$

In this representation, the correlator satisfies

$$\partial_t \hat{S}(k, t) = -k^2 \left(D \hat{S}(k, t) + \int_0^t ds \hat{M}(k, s) \hat{S}(k, t - s) \right) \quad (7.2)$$

with memory kernel

$$\hat{M}_{\alpha\alpha'}(k, s) = 2 \int_{\mathbb{R}} dq \operatorname{tr} \left[G^\alpha \hat{S}(k - q, s)^\top G^{\alpha'} \hat{S}(q, s) \right]. \quad (7.3)$$

Eq. (7.2) has to be solved with the initial condition

$$\hat{S}(k, 0) = 1, \quad (7.4)$$

reflecting the sum rule (2.15) and $C = 1$. One notes that Eq. (7.2) is preserved under rotations, i.e. $\tilde{S} = RSR^\top$ satisfies again Eq. (7.2) with \vec{G} replaced by $\vec{\tilde{G}}$.

In the long time limit, the solution is expected to be of self-similar form as

$$\hat{S}_{\alpha\beta}(k, t) \simeq F_{\alpha\beta}(t^{2/3}k), \quad F_{\alpha\beta}(0) = \delta_{\alpha\beta}. \quad (7.5)$$

Under this scaling the diffusive term (7.2) is subleading and hence can be omitted. However, it might become relevant for special choices of \vec{G} . Assuming the approximation (7.5) and setting $w = t^{2/3}k$, the scaling matrix F satisfies

$$\frac{2}{3}w \frac{d}{dw} F(w) = -w^2 \int_0^1 ds \mathbf{M}(w, s) F((1-s)^{2/3}w), \quad (7.6)$$

with initial condition $F(0) = 1$, where

$$\mathbf{M}_{\alpha\alpha'}(w, s) = 2 \int_{\mathbb{R}} dq \operatorname{tr} \left[G^\alpha F(s^{2/3}(w - q))^\top G^{\alpha'} F(s^{2/3}q) \right]. \quad (7.7)$$

Note that F is even, $F(w) = F(-w)$.

In principle, $F(w)$ can be obtained by solving Eq. (7.2) numerically through iteration, properly including the memory kernel, and taking the long time limit [19]. We have not pursued this direction any further, but focus on the specific model discussed in Section 3. For this model the off-diagonal matrix elements, $\hat{S}_{12}, \hat{S}_{21}$, vanish. Such property is correctly reproduced by mode-coupling and Eq. (7.6) simplifies to two coupled equations for F_{11} and F_{22} , which read

$$\begin{aligned} \frac{1}{3}w \frac{d}{dw} F_{11}(w) &= -2w^2 \int_0^1 ds \mathbf{M}[F_{11}, F_{22}](w, s) F_{11}((1-s)^{2/3}w), \\ \frac{1}{3}w \frac{d}{dw} F_{22}(w) &= -w^2 \int_0^1 ds \left(\mathbf{M}[F_{11}, F_{11}](w, s) + \lambda^2 \mathbf{M}[F_{22}, F_{22}](w, s) \right) F_{22}((1-s)^{2/3}w), \end{aligned} \quad (7.8)$$

where $\mathbf{M}[f, \tilde{f}]$ is defined by

$$\mathbf{M}[f, \tilde{f}](w, s) = 2 \int_{\mathbb{R}} dq f(s^{2/3}(w - q)) \tilde{f}(s^{2/3}q). \quad (7.9)$$

As a shortcoming, the solution depends only on λ^2 , which is not the case for the stochastic Burgers equation, compare with the discussion at the end of Section 4.

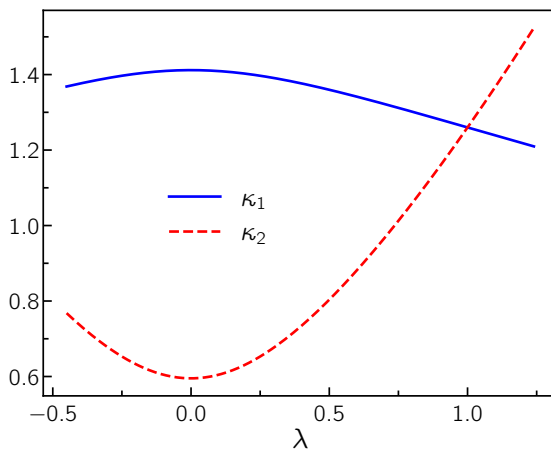


Figure 8: Plots for κ_1 and κ_2 versus λ obtained by solving Eq. (7.11) numerically. At $\lambda = 1$, the fixed point is $\kappa_1 = \kappa_2 = 2^{1/3}$. Decreasing λ , the κ 's are varying with $\kappa_1 < \kappa_2$, in qualitative agreement with the plots in Fig. 1. The κ 's are even functions with maximal distance at $\lambda = 0$.

The solution is still complicated and we try the simple-minded ansatz

$$F_{11}(w) = \exp(-c\kappa_1 w^2), \quad F_{22}(w) = \exp(-c\kappa_2 w^2), \quad F_{12}(w) = 0 = F_{21}(w) \quad (7.10)$$

with some coefficients $c, \kappa_1, \kappa_2 > 0$. This expression is inserted in Eqs. (7.8), (7.9). An equation for κ_1, κ_2 is obtained by evaluating right and left hand side at $w = 0$. Choosing the scale parameter c according to maximal simplicity, the result reads

$$\kappa_1 = 2 \frac{1}{\sqrt{\kappa_1 + \kappa_2}}, \quad \kappa_2 = \frac{1}{\sqrt{2\kappa_1}} + \lambda^2 \frac{1}{\sqrt{2\kappa_2}}. \quad (7.11)$$

For $\lambda = 1$ the solution is $\kappa_1 = \kappa_2$, as it should be and $\kappa_1 = 2^{1/3}$. As can be seen in Fig. 8 as λ varies the Gaussian scaling functions vary smoothly. At $\lambda = 0$ the separation of curves is maximal. Considering the ratio of the maximal heights in x space, one obtains 1.52 on the basis of (7.11), while Fig. 1 yields 1.89. A numerical solution of the full mode-coupling equations presumably will do even better.

A slightly more sophisticated argument comes from the observation that at $\lambda = 1$, one has $F_{11} = F_{22} = F_0$, where F_0 is the fixed point for the one-component mode-coupling equation, which is numerically known with good precision [19]. One can then expand around this solution. To first order one obtains non-vanishing corrections to F_0 . This further supports that within mode-coupling the scaling functions have a nontrivial dependence on λ .

8. Discussions

Relation to the work of Ertas-Kardar [21, 22]: Using our notation, after transformation to $C = 1$, the model considered in [21] has the G^α matrices

$$G^1 = \begin{pmatrix} 0 & b \\ b & 0 \end{pmatrix}, \quad G^2 = \begin{pmatrix} \tilde{b} & 0 \\ 0 & d \end{pmatrix}. \quad (8.1)$$

Cyclicity would require $b = \tilde{b}$, which then corresponds to the line marked by stars in Fig. 2 of [21]. At the time, only scaling exponents were studied. On the other hand, cyclic matrices are only a line in their phase diagram. Thus it would be of interest to explore also stochastic Burgers equations with non-cyclic coupling matrices.

Isotropic spin chains: The $t^{\frac{2}{3}}$ scaling of the spin-spin correlation has been observed earlier for classical integrable isotropic spin chains [25] and in DMRG simulations of a discretized version of the isotropic Heisenberg chain [11]. Furthermore, the scaling function shows excellent agreement with the scaling function f_{KPZ} from the single component Burgers equation. Eq. (3.1) with $b = \frac{1}{2}$ was derived in [14] as an effective stochastic theory for spin and helicity density of the spin-spin spacetime correlation function of the XXX spin- $\frac{1}{2}$ Heisenberg chain. As in the current contribution, the authors investigate the issue of universality when varying the parameter λ . Our numerical simulations indicate that, while the 3/2 KPZ exponent is confirmed, there are discrepancies from the single component KPZ scaling form. Similarly, for time-integrated currents, we observe deviations from the Baik-Rains distribution. It is therefore of interest to revisit the issue of an effective stochastic description of isotropic quantum spin chains [50].

Beta log-gas: As one of our central findings, the coupled systems under consideration have KPZ exponent but coupling-dependent scaling functions. Although exceptional such features are known from other models in statistical mechanics. One example is the one-dimensional repulsive log gas with strength parameter β . At $\beta = 2$, the Gibbs measure is the joint probability density of the N eigenvalues of a GUE random matrix. The spatial scale is chosen such that the edge of the density of states equals $2N$, i.e. the typical distance of eigenvalues is of order 1. Considering the largest eigenvalue, it is order $N^{\frac{1}{3}}$ away from the edge. For $\beta = 2$, at large N the limiting distribution is Tracy-Widom [51]. Now varying β , the scaling exponent $\frac{1}{3}$ stays put, but the asymptotic probability density for the largest eigenvalue depends on β [52, 53].

9. Summary and Outlook

In our contribution, the KPZ scaling theory is extended to stochastic dynamics with two conservation laws possessing a degenerate flux Jacobian. The structure function is then a 2×2 matrix and its two peaks have the same velocity. The theory is applied to the steady state spacetime correlator and time-integrated current across the origin. Numerically compared is the long time asymptotics of a two-lane stochastic lattice gas and a continuum coupled stochastic Burgers equation. Our central innovation relies on a similarity transform of the static susceptibility matrix. In our simulations, the dynamical scaling exponent $3/2$ is confirmed with great precision. The form of the scaling functions, however, cannot be explained in terms of what one knows about the one-component case.

Many interesting problems remain yet to be explored. We have investigated only a single parameter value. Hence the most immediate issue is a better understanding of scaling functions for two-component systems at the umbilic point. From a theoretical perspective, for a single component the steady state is expected to have a finite correlation length. For two components, away from cyclicity, this might no longer be valid. If so, the dynamical exponent might change. A further point concerns two-component lattice gases. The two-lane model studied here seems to be one of the very few examples allowing for degeneracy of the flux Jacobian. Another interesting example is a system comprising of sliding particles on a fluctuating landscape [54, 55]. It would be of interest to enlarge the class of such models.

Acknowledgements

HS greatly benefited from discussions with Jacopo De Nardis and thanks Fabio Toninelli for mentioning the Beta log-gas. DR, AD and MK acknowledge support from the Department of Atomic Energy, Government of India, under Project No. RTI4001. KK thanks Alexander von Humboldt Foundation for their support which made his visit to Munich possible. KK and MK thank the hospitality of the Department of Mathematics of the Technical University of Munich, Garching (Germany). AD, MK and HS thank the VAJRA faculty scheme (No. VJR/2019/000079) from the Science and Engineering Research Board (SERB), Department of Science and Technology, Government of India.

Appendix A.

Transforming \vec{G} -matrices

We start from two general matrices G^1, G^2 satisfying the cyclicity condition,

$$G^1 = \begin{pmatrix} a & b \\ b & c \end{pmatrix}, \quad G^2 = \begin{pmatrix} b & c \\ c & d \end{pmatrix}. \quad (\text{A.1})$$

Then under rotations they transform to \tilde{G}^α , which explicitly are given by

$$\begin{aligned} \tilde{G}_{11}^1 &= a \cos^3 \vartheta + 3b \cos^2 \vartheta \sin \vartheta + 3c \cos \vartheta \sin^2 \vartheta + d \sin^3 \vartheta, \\ \tilde{G}_{12}^1 &= \tilde{G}_{21}^1 = b \cos^3 \vartheta + (-a + 2c) \cos^2 \vartheta \sin \vartheta + (-2b + d) \cos \vartheta \sin^2 \vartheta - c \sin^3 \vartheta, \\ \tilde{G}_{22}^1 &= c \cos^3 \vartheta + (-2b + d) \cos^2 \vartheta \sin \vartheta + (a - 2c) \cos \vartheta \sin^2 \vartheta + b \sin^3 \vartheta \end{aligned} \quad (\text{A.2})$$

and

$$\begin{aligned} \tilde{G}_{11}^2 &= b \cos^3 \vartheta + (-a + 2c) \cos^2 \vartheta \sin \vartheta + (-2b + d) \cos \vartheta \sin^2 \vartheta - c \sin^3 \vartheta, \\ \tilde{G}_{12}^2 &= \tilde{G}_{21}^2 = c \cos^3 \vartheta + (-2b + d) \cos^2 \vartheta \sin \vartheta + (a - 2c) \cos \vartheta \sin^2 \vartheta + b \sin^3 \vartheta, \\ \tilde{G}_{22}^2 &= d \cos^3 \vartheta - 3c \cos^2 \vartheta \sin \vartheta + 3b \cos \vartheta \sin^2 \vartheta - a \sin^3 \vartheta. \end{aligned} \quad (\text{A.3})$$

By inspection \tilde{G}^α are still cyclic. Setting either $b, c, d = 0$ or $a, b, c = 0$ yields (2.30) and (2.31).

Appendix B.

Further results for the two-lane model

Appendix B.1.

Cyclicity

To merely find out about cyclicity, we can also check the one of \hat{H}^α . The inverse of C is given by

$$C^{-1} = \frac{1}{2\Omega - 4\Omega^2} \begin{pmatrix} 1 & 1 - 4\Omega \\ 1 - 4\Omega & 1 \end{pmatrix}. \quad (\text{B.1})$$

Using the definition (2.12) one obtains

$$\hat{H}^1 = (C^{-1})_{11} H^1 + (C^{-1})_{12} H^2, \quad \hat{H}^2 = (C^{-1})_{21} H^1 + (C^{-1})_{22} H^2. \quad (\text{B.2})$$

Cyclicity follows by inserting \vec{H} from (4.9) and using the identity (4.10) for Ω .

Appendix B.2.

Uniqueness of the umbilic point

It is convenient to switch to new coordinates

$$w = \frac{1}{2} - u, \quad y = \frac{1}{2} - v \quad (\text{B.3})$$

with $|w| < \frac{1}{2}, |y| < \frac{1}{2}$. Then

$$A = \begin{pmatrix} 2w - y & -w \\ y & w - 2y \end{pmatrix} + \kappa \begin{pmatrix} y + \frac{1}{2}q(w + y) & w + \frac{1}{2}q(w + y) \\ -y - \frac{1}{2}q(w + y) & -w - \frac{1}{2}q(w + y) \end{pmatrix}, \quad (\text{B.4})$$

where

$$\kappa = \frac{1}{\sqrt{f}}, \quad f(w, y) = 1 + q + q^2(w + y)^2 + 4qwy. \quad (\text{B.5})$$

Proved is the following

Lemma. If $q > -1$ and $q \neq 0$, then $u = \frac{1}{2} = v$ is the unique umbilic point of the flux Jacobian A .

Proof: We consider the characteristic polynomial of A . Its discriminant is given by

$$D = (A_{11} - A_{22})^2 + 4A_{12}A_{21}. \quad (\text{B.6})$$

One knows already that $D \geq 0$. To be established is $D = 0$ only if $w = 0 = y$.

One computes

$$D = (1 + \kappa + q\kappa)^2(w + y)^2 + 2q\kappa(1 - \kappa - \frac{1}{2}q\kappa)(w^2 + y^2) - 4\left(\frac{1}{4}q^2\kappa^2 + (1 - \kappa - \frac{1}{2}q\kappa)^2\right)wy. \quad (\text{B.7})$$

Clearly, D is a quadratic form in w, y , which defines the 2×2 matrix E . It remains to show that $E > 0$, which is implied by $\text{tr}E > 0$ and $\det E > 0$. Now

$$\text{tr}E = (1 + \kappa)^2 + 4q\kappa, \quad \det E = 16(1 + q)\kappa(1 - \kappa)^2. \quad (\text{B.8})$$

For $q > -1$ and $\kappa > 0$, one concludes that $\text{tr}E > 0$. The determinant can vanish only at $\kappa = 1$. Thus we have to discuss the solution of $1 + q(w + y)^2 + 4wy = 0$. Its only solutions are $\frac{1}{2}(1, -1), \frac{1}{2}(-1, 1)$. In the interior of the quadrant the left hand side is strictly positive and thus $\det E > 0$.

Appendix C.

Symmetric and anti-symmetric combinations

If one considers Eq. (3.1) at $\lambda = 1$, it is easy to show that symmetric and anti-symmetric combinations, $\phi_{\pm} = (\phi_2 \pm \phi_1)/\sqrt{2}$, decouple into two independent stochastic Burgers equations. Hence one may wonder how ϕ_{\pm} changes when $\lambda \neq 1$. In Fig. C1, we show spacetime correlations and current fluctuations for the symmetric combination at $\lambda = 0$. The spacetime correlation is defined by

$$S_{++}(x, t) = \langle \phi_+(x, t)\phi_+(0, 0) \rangle. \quad (\text{C.1})$$

and the current fluctuation are obtained using

$$\zeta_{\pm} = (\zeta_2 \pm \zeta_1)/\sqrt{2}. \quad (\text{C.2})$$

We see that although KPZ exponent is confirmed the scaling functions and current distributions differ significantly from the single component stochastic Burgers equation. Therefore, the case $\lambda \neq 1$ is not equivalent to two independent Burgers equations as seems to have been suggested in [14].

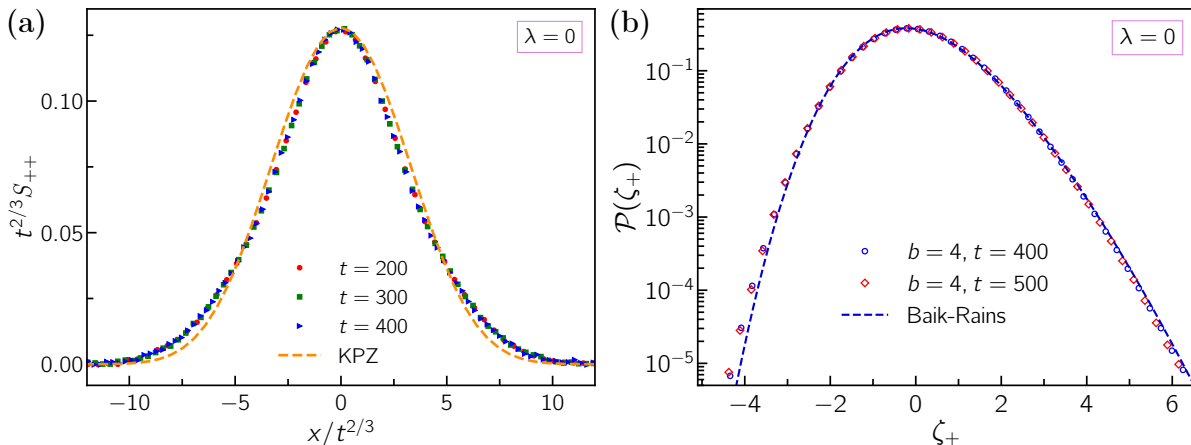


Figure C1: Plots of (a) the spacetime correlation S_{++} (C.1) and (b) the PDF (C.2) for the height fluctuations ζ_+ corresponding to the field $\phi_+ = (\phi_1 + \phi_2)/\sqrt{2}$. The spacetime correlation for $\phi_- = (-\phi_1 + \phi_2)/\sqrt{2}$ is the same as S_{++} . Also, the distributions of the height fluctuations corresponding to ϕ_+ and ϕ_- are same (see Table 1) owing to the symmetry $h_1 \rightarrow -h_1$.

References

- [1] Mehran Kardar, Giorgio Parisi, and Yi-Cheng Zhang. Dynamic scaling of growing interfaces. *Physical Review Letters*, 56:889, 1986.
- [2] Timothy Halpin-Healy and Yi-Cheng Zhang. Kinetic roughening phenomena, stochastic growth, directed polymers and all that. aspects of multidisciplinary statistical mechanics. *Physics Reports*, 254:215, 1995.
- [3] Ivan Corwin. The Kardar-Parisi-Zhang equation and universality class. *Random Matrices: Theory and Applications*, 01:1130001, 2012.
- [4] Bernard Derrida. An exactly soluble non-equilibrium system: the asymmetric simple exclusion process. *Physics Reports*, 301:65, 1998.

- [5] Bernard Derrida, Martin R Evans, Vincent Hakim, and Vincent Pasquier. Exact solution of a 1D asymmetric exclusion model using a matrix formulation. *Journal of Physics A: Mathematical and General*, 26:1493, 1993.
- [6] Vladislav Popkov and Gunter M Schütz. Shocks and excitation dynamics in a driven diffusive two-channel system. *Journal of Statistical Physics*, 112:523, 2003.
- [7] Richard A Blythe and Martin R Evans. Nonequilibrium steady states of matrix-product form: a solver’s guide. *Journal of Physics A: Mathematical and Theoretical*, 40:R333, 2007.
- [8] Michael Prähofer and Herbert Spohn. Scale invariance of the PNG droplet and the Airy process. *Journal of Statistical Physics*, 108:1071, 2002.
- [9] Herbert Spohn. Nonlinear fluctuating hydrodynamics for anharmonic chains. *Journal of Statistical Physics*, 154:1191, 2014.
- [10] Marko Žnidarič. Spin transport in a one-dimensional anisotropic Heisenberg model. *Physical Review Letters*, 106:220601, 2011.
- [11] Marko Ljubotina, Marko Žnidarič, and Tomaž Prosen. Kardar-Parisi-Zhang physics in the quantum Heisenberg magnet. *Physical Review Letters*, 122:210602, 2019.
- [12] A. Scheie, N. E. Sherman, M. Dupont, S. E. Nagler, M. B. Stone, G. E. Granroth, J. E. Moore, and D. A. Tennant. Detection of Kardar–Parisi–Zhang hydrodynamics in a quantum Heisenberg spin-1/2 chain. *Nature Physics*, 17:726, 2021.
- [13] David Wei, Antonio Rubio-Abadal, Bingtian Ye, Francisco Machado, Jack Kemp, Kritsana Srakaew, Simon Hollerith, Jun Rui, Sarang Gopalakrishnan, Norman Y. Yao, Immanuel Bloch, and Johannes Zeiher. Quantum gas microscopy of Kardar-Parisi-Zhang superdiffusion. *Science*, 376:716, 2022.
- [14] Jacopo De Nardis, Sarang Gopalakrishnan, and Romain Vasseur. Nonlinear fluctuating hydrodynamics for Kardar-Parisi-Zhang scaling in isotropic spin chains. *Physical Review Letters*, 131:197102, 2023.
- [15] Herbert Spohn. The Kardar–Parisi–Zhang equation: a statistical physics perspective. In *Stochastic Processes and Random Matrices: Lecture Notes of the Les Houches Summer School: Volume 104, July 2015*. Oxford University Press, 2017.
- [16] Kazumasa A. Takeuchi. An appetizer to modern developments on the Kardar-Parisi-Zhang universality class. *Physica A: Statistical Mechanics and its Applications*, 504:77, 2018. Lecture Notes of the 14th International Summer School on Fundamental Problems in Statistical Physics.
- [17] Rafael M Grisi and Gunter M Schütz. Current symmetries for particle systems with several conservation laws. *Journal of Statistical Physics*, 145:1499, 2011.
- [18] Patrik L Ferrari, Tomohiro Sasamoto, and Herbert Spohn. Coupled Kardar-Parisi-Zhang equations in one dimension. *Journal of Statistical Physics*, 153:377, 2013.
- [19] Christian B. Mendl and Herbert Spohn. Dynamic correlators of Fermi-Pasta-Ulam chains and nonlinear fluctuating hydrodynamics. *Physical Review Letters*, 111:230601, 2013.
- [20] Suman G. Das, Abhishek Dhar, Keiji Saito, Christian B. Mendl, and Herbert Spohn. Numerical test of hydrodynamic fluctuation theory in the Fermi-Pasta-Ulam chain. *Physical Review E*, 90:012124, 2014.
- [21] Deniz Ertaş and Mehran Kardar. Dynamic relaxation of drifting polymers: A phenomenological approach. *Physical Review E*, 48:1228, 1993.
- [22] Deniz Ertaş and Mehran Kardar. Dynamic roughening of directed lines. *Physical Review Letters*, 69:929, 1992.
- [23] Jeremy Quastel and Herbert Spohn. The one-dimensional KPZ equation and its universality class. *Journal of Statistical Physics*, 160:965, 2015.

- [24] Tomaž Prosen and Bojan Žunkovič. Macroscopic diffusive transport in a microscopically integrable hamiltonian system. *Physical Review Letters*, 111:040602, 2013.
- [25] Avijit Das, Manas Kulkarni, Herbert Spohn, and Abhishek Dhar. Kardar-Parisi-Zhang scaling for an integrable lattice Landau-Lifshitz spin chain. *Physical Review E*, 100:042116, 2019.
- [26] Žiga Krajnik and Tomaž Prosen. Kardar-Parisi-Zhang physics in integrable rotationally symmetric dynamics on discrete space-time lattice. *Journal of Statistical Physics*, 179:110, 2020.
- [27] Žiga Krajnik, Enej Ilievski, and Tomaž Prosen. Integrable Matrix Models in Discrete Space-Time. *SciPost Physics*, 9:38, 2020.
- [28] Bingtian Ye, Francisco Machado, Jack Kemp, Ross B. Hutson, and Norman Y. Yao. Universal Kardar-Parisi-Zhang dynamics in integrable quantum systems. *Physical Review Letters*, 129:230602, 2022.
- [29] Google Quantum AI and Collaborators. Dynamics of magnetization at infinite temperature in a Heisenberg spin chain. *arXiv:2306.09333*, 2023.
- [30] Vladislav Popkov, Johannes Schmidt, and Gunter M. Schütz. Superdiffusive modes in two-species driven diffusive systems. *Physical Review Letters*, 112:200602, 2014.
- [31] Michael Prähofer and Herbert Spohn. Exact scaling functions for one-dimensional stationary KPZ growth. *Journal of Statistical Physics*, 115:255, 2004.
- [32] Patrik L Ferrari and Herbert Spohn. Scaling limit for the space-time covariance of the stationary totally asymmetric simple exclusion process. *Communications in Mathematical Physics*, 265:1, 2006.
- [33] Alexei Borodin, Ivan Corwin, Patrik Ferrari, and Bálint Vető. Height fluctuations for the stationary KPZ equation. *Mathematical Physics, Analysis and Geometry*, 18:1, 2015.
- [34] Tadahisa Funaki. Infinitesimal invariance for the coupled KPZ equations. In Catherine Donati-Martin, Antoine Lejay, and Alain Rouault, editors, *In Memoriam Marc Yor - Séminaire de Probabilités XLVII*, page 37. Springer International Publishing, Cham, 2015.
- [35] Tomohiro Sasamoto and Herbert Spohn. Superdiffusivity of the 1D lattice Kardar-Parisi-Zhang equation. *Journal of Statistical Physics*, 137:917, 2009.
- [36] Kohei Hayashi. Derivation of coupled KPZ equations from interacting diffusions driven by a single-site potential. *arXiv:2208.05374*, 2023.
- [37] Tadahisa Funaki and Masato Hoshino. A coupled KPZ equation, its two types of approximations and existence of global solutions. *Journal of Functional Analysis*, 273:1165, 2017.
- [38] Joachim Krug and Paul Meakin. Universal finite-size effects in the rate of growth processes. *Journal of Physics A: Mathematical and General*, 23:L987, 1990.
- [39] Joachim Krug, Paul Meakin, and Timothy Halpin-Healy. Amplitude universality for driven interfaces and directed polymers in random media. *Physical Review A*, 45:638, 1992.
- [40] Christian B. Mendl and Herbert Spohn. Searching for the Tracy-Widom distribution in nonequilibrium processes. *Physical Review E*, 93:060101, 2016.
- [41] Jinho Baik and Eric M Rains. Limiting distributions for a polynuclear growth model with external sources. *Journal of Statistical Physics*, 100:523, 2000.
- [42] Michael Prähofer and Herbert Spohn. Universal distributions for growth processes in 1+1 dimensions and random matrices. *Physical Review Letters*, 84:4882, 2000.
- [43] Peter F Arndt, Thomas Heinzl, and Vladimir Rittenberg. Spontaneous breaking of translational invariance in one-dimensional stationary states on a ring. *Journal of Physics A: Mathematical and General*, 31:L45, 1998.
- [44] Peter F Arndt, Thomas Heinzl, and Vladimir Rittenberg. Spontaneous breaking of translational invariance and spatial condensation in stationary states on a ring. I. the neutral system. *Journal*

- of *Statistical Physics*, 97:1, 1999.
- [45] Cédric Bernardin and Gabriel Stoltz. Anomalous diffusion for a class of systems with two conserved quantities. *Nonlinearity*, 25:1099, 2012.
 - [46] Herbert Spohn and Gabriel Stoltz. Nonlinear fluctuating hydrodynamics in one dimension: The case of two conserved fields. *Journal of Statistical Physics*, 160:861, 2015.
 - [47] Henk van Beijeren. Exact results for anomalous transport in one-dimensional Hamiltonian systems. *Physical Review Letters*, 108:180601, 2012.
 - [48] Vladislav Popkov and Gunter M. Schütz. Unusual shock wave in two-species driven systems with an umbilic point. *Physical Review E*, 86:031139, 2012.
 - [49] Henk van Beijeren, Ryszard Kutner, and Herbert Spohn. Excess noise for driven diffusive systems. *Physical Review Letters*, 54:2026, 1985.
 - [50] Žiga Krajnik, Johannes Schmidt, Enej Ilievski, and Tomaž Prosen. Dynamical criticality of magnetization transfer in integrable spin chains. *Physical Review Letters*, 132:017101, 2024.
 - [51] Kurt Johansson. Shape fluctuations and random matrices. *Communications in Mathematical Physics*, 209:437, 2000.
 - [52] Jose Ramirez, Brian Rider, and Bálint Virág. Beta ensembles, stochastic Airy spectrum, and a diffusion. *Journal of the American Mathematical Society*, 24:919, 2011.
 - [53] Peter J Forrester. *Log-gases and random matrices*. Princeton University Press, 2010.
 - [54] Shaurya Chakraborty, Sakuntala Chatterjee, and Mustansir Barma. Ordered phases in coupled nonequilibrium systems: Static properties. *Physical Review E*, 96:022127, 2017.
 - [55] Shaurya Chakraborty, Sakuntala Chatterjee, and Mustansir Barma. Dynamics of coupled modes for sliding particles on a fluctuating landscape. *Physical Review E*, 100:042117, 2019.